Investigation of Sol−Gel Transition in Pluronic F127/D_2O Solutions Using a Combination of Small-Angle Neutron Scattering and Monte Carlo Simulation

Yunqi Li,[†,‡] Tongfei Shi,[‡] Zhaoyan Sun,[‡] Lijia An,*[,‡] and Qingrong Huang*[,†]

Department of Food Science, Rutgers University, 65 Dudley Road, New Brunswick, New Jersey 08901, and State Key Laboratory of Polymer Physics and Chemistry, Changchun Institute of Applied Chemistry, Chinese Academy of Sciences, Changchun 130022, People's Republic of China

Received: September 15, 2006; In Final Form: October 23, 2006

Physical gelation in the concentrated Pluronic F127/D_2O solution has been studied by a combination of small-angle neutron scattering (SANS) and Monte Carlo simulation. A 15% F127/D_2O solution exhibits a sol−gel transition at low temperature and a gel-sol transition at the higher temperature, as evidenced by SANS and Monte Carlo simulation studies. Our SANS and simulation results also suggest that the sol−gel transition is dominated by the formation of a percolated polymer network, while the gel−sol transition is determined by the loss of bound solvent. Furthermore, different diffusion behaviors of different bound solvents and free solvent are observed. We expect that this approach can be further extended to study phase behaviors of other systems with similar sol−gel phase diagrams.

Introduction

Physical gelation in polymer solutions by self-assembly of polymer chains has attracted intensive studies during the past 20 years. Polymeric gels have been widely used in drug delivery applications, microstructured materials templates, nutrient stabilization, and in cosmetics and food-related applications.[1,2] On the other hand, fundamental understanding of the physical gelation, including the structure and properties, as well as their relationship of the gels, the gelation mechanism, and the sol−gel phase diagrams, is always an active topic in soft condensed matter. Although many works have been published to reveal the nature of physical gelation in polymer solutions,[3,4] there is no unique approach that can well describe the gelation in both the synthetic copolymer solutions and the natural biopolymer solutions. The percolation theory[5] has been established to explain most of the gelation phenomena, but some researchers argue that the physical gelation is beyond percolation.[6] The scaling theory[7] affords a universal mathematic expression for physical gelation, but it is far away from illustrating the nature of the physical gelation.

In this work, we propose an approach that can be used to understand the nature of physical gelation in different kinds of polymer solutions. On the basis of the origin of the viscoelastic properties of physical gels in which polymer networks exhibit solidlike elastic properties and the solvents exhibit liquidlike viscous properties, we consider two important aspects in the physical gelation process: (1) the formation of percolated polymer gel network, and (2) the formation of a percolated system that requires the volume fraction of the bound solvent exceeding a critical value. This approach has been used to explain the results from small-angle neutron scattering (SANS) studies on the temperature and concentration induced physical gelation in the triblock copolymer Pluronic F127/D_2O solution, and Monte Carlo simulation based on the features of F127/D_2O solution.

Experimental Section

The Pluronic F127 ($EO_{100}PO_{65}EO_{100}$ in which EO refers to ethylene oxide and PO refers to propylene oxide) was obtained from BASF Corp., New Jersey, and was used without further purification. The solutions were prepared by dissolving F127 of different concentrations into D_2O (99.9% deuterium, Aldrich). The SANS experiments were performed at the intense pulsed neutron source at Argonne National Laboratory (ANL) using a time-of-flight small angle diffractometer (SASI).[8] The SASI instrument uses a multiple-aperture collimator consisting of a crossed pair of converging Soller collimators, one for vertical definition and the other for horizontal definition of the angular distribution, with the wavelength resolution $\Delta\lambda/\lambda$ ranging from 5 to 25%. Two millimeter quartz cells were used throughout the experiments, and data was collected over 1 h at each temperature and concentration. A liquid flow thermostat was used to control the temperature to within $\pm$ 1 °C. All the data were recorded in the q-range of 0.005−1 $Å^{-1}$ and corrected for detector efficiency, solvent scattering, and sample transmission. The raw data were deduced following the procedures described by Thiyagarajan et al.,[8] and the incoherent scattering intensity was treated at a large q-range using the method introduced by Hansen and Pedersen.[9] The scattering intensity profiles were shown within partial q-ranges to minimize the distraction from the intensity fluctuations at small and large q-ranges.

Monte Carlo Simulations

In the Monte Carlo simulation, the structure of the triblock copolymer was set as $A_{21}B_{18}A_{21}$, where A and B represented the coarse-grained segments of EO and PO respectively. The subscript number represented the number of segments in each block. When the temperature-dependent interactions in F127/D_2O solutions were taken into account, the interaction terms were set as: $\epsilon_{AS} = -0.5k_BT/T^*$, and $\epsilon_{BB} = -\epsilon_{BS} = -0.5k_BT$

* To whom all correspondence should be addressed. (Q.H.) Email: qhuang@aesop.rutgers.edu. Tel: 732-932-7193. Fax: 732-932-6776. (L.A.) E-mail: ljan@ciac.jl.cn. Tel.: +86-431-5262296. Fax: +86-431-5685653.
† Rutgers University.
‡ Changchun Institute of Applied Chemistry.

10.1021/jp066019r CCC: $33.50 © 2006 American Chemical Society
Published on Web 12/01/2006

$\times T^*$, where T^* was the reduced temperature which varied from 0.1 to 10, corresponding to the decrease of solvent quality when the temperature increases in the F127/D_2O solution. In our experiments, when the temperature ranges from 22 to 80 °C, the D_2O is always a good solvent for EO segments, but the solvent quality decreases as the temperature increases. The interaction ϵ_{AS} represents the interaction between the EO segments and D_2O, which decreases with the increase of T^* but still maintains weak attractive interaction, suggesting that the solvent is always a good solvent for A segments in the simulation. It has been reported that water is a good solvent for PO for temperature up to 15 °C.[10] Therefore, in our experimental temperature range, D_2O is not a good solvent for PO segments, and the hydrophobic interaction dominates the interaction between PO segments and D_2O. This interaction becomes stronger when the temperature gets higher. To model the hydrophobic interaction and temperature effect, Anderson and Travesset have successfully described the interaction between EO and water with the variation of temperature by separating the hydrophobic interaction into a repulsive interaction and an attractive interaction.[11]

In this work, the hydrophobic interaction was treated by ϵ_{BB} and ϵ_{BS}, which included an attractive interaction between PO segments and a repulsive interaction between PO segments and D_2O. Both the attractive and repulsive interactions increased with temperature. The volume fraction of the triblock copolymer ϕ changed from 0.05 to 0.30, and the simulation lattice was set as $L \times L \times L$ with $L = 128$. Periodic boundary condition was imposed on each direction of the simulation lattice to eliminate the finite box size effect. The Monte Carlo simulation was preformed using a lattice model, which was based on the eight-site model[12] in which each segment occupied a small cube, and the bond fluctuation algorithm[13] was used for the thermodynamic relaxation of the simulation lattice that allowed the bond length of two consecutive segments to fluctuate in $\{2, \sqrt{5}, \sqrt{6}, 3, \sqrt{10}\}$.

The coarse-grain keeps the mass density homogeneous in the simulation lattice, that is, one small cube represents 4.76 EO monomers, 3.61 PO monomers, and 10.47 D_2O molecules when it is occupied by A, B, and S (coarse grained segment of solvent) respectively, and thus the coherent scattering length density is 2.72, 1.25, and 86.28 ($\times 10^4$ cm^{-2}) for the A, B, and S occupied sites, respectively.[14] Twenty parallel samples with different initial configurations and random sequences have been calculated to achieve accurate results and to determine the sol−gel phase diagram using the method introduced in our previous work,[15,16] except that the criteria of gelation used in this work are different. There are two criteria used in this work including (1) the formation of percolated polymer networks, which can be achieved through a combination of the site percolation of PO−PO interaction (nearest neighboring interactions among the sites occupied by segment B) and the bond percolation along the copolymer chains, and (2) the volume fraction of the bound solvents exceeding a critical value, which is taken as 0.16 according to the literature reports,[17] for random networks built up by individual units. Each simulation sample has run 5×10^6 Monte Carlo steps (MCS) for thermodynamic relaxation, and the total interaction energy in each sample saturates with MCS (figure not shown), suggesting that these samples are under thermodynamic equilibrium. The error bars are not bigger than the symbol sizes of the results and therefore are not specifically shown in the figures.

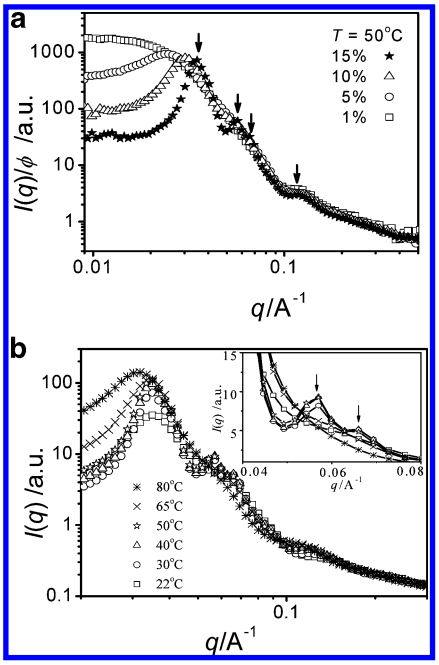

Figure 1. The plots of concentration-normalized SANS intensity profiles versus F127 concentrations for F127/D_2O solutions at 50 °C (a), and the temperature-dependent scattering intensity profiles at 15 wt % F127/D_2O solution (b). The inset of (b) is the enlargement of the peaks at q-range of 0.04∼0.08 Å^{-1}. The arrows in (a) on the 15% curve, from left to right, indicate the peak positions at around 0.034, 0.057, 0.067, and 0.121 Å^{-1} respectively, while the arrows in the inset of (b) correspond to the peak positions at around 0.057 and 0.067 Å^{-1} respectively.

Results and Discussions

The gelation in F127/D_2O solutions studied by SANS has been extensively reported by other groups.[18] However, the investigation of the scattering intensity profiles [$I(q)$ vs q] with such large concentration and temperature ranges as in this work has not been reported before. All the data reported in this paper are in the concentration ranges above the critical micelle concentration.[19,20] The micellar structures of PEO-PPO-PEO triblock copolymers in dilute aqueous solutions are quite clear:[10,21] with the increase of copolymer concentration and temperature, the copolymer chains initially form spherical micelles consisting of hydrophobic cores surrounded by hydrophilic coronas. For the scattering results, the micellar core can be described using hard sphere form factor, and the coronas can be described using the form factor of Gaussian coil.[22,23] Further increase of temperature results in the dehydration of the hydrophilic EO blocks and the decrease of solubility for the hydrophobic PO blocks, causing the sizes of the hydrophobic core to increase and leading to the formation of a rodlike structure. However, the physical properties of F127 at high concentration still remain controversial.

In this paper, we limit our focus on the understanding of the concentration-induced gel formation and temperature-induced sol−gel and gel−sol transitions in F127/D_2O solutions. Several characteristics can be observed in Figure 1a, which shows the concentration dependent SANS intensity profiles of F127 in D_2O solutions at 50 °C: (i) A broad shoulder at q-range of 0.1∼0.13 Å^{-1}, which is due to intraparticle interference, always exists, revealing that the micelle core sizes are about 4.8∼6.3 nm and independent of concentration, consistent with previous reports.[18,20,24] (ii) For 5% 127 solution, which is below the gelation threshold, only an interparticle peak centered at a q-range of 0.03∼0.04 Å^{-1} appears, and no higher order diffraction peaks

appear, suggesting the absence of supramicellar structures.[25,26] The interparticle peak shifts to a higher q value with the further increase of F127 concentration to 15 wt %, indicating that the higher polymer concentration leads to a shorter intermicellar distance. (iii) With the further increase of F127 concentration to 15%, a secondary peak ($q \approx 0.057$ Å^{-1}) and a small shoulder peak ($q \approx 0.067$ Å^{-1}; this can be seen more clearly from the inset of Figure 1b) at a q-range of 0.05∼0.07 Å^{-1} appear. Combining our SANS results with the reported rheology studies[25] and the phase diagram of F127 in aqueous solutions,[19] we interpret these peaks, which correspond to the short-range correlation, as resulting from the gel formation, similar to the reported physical gelation from other systems.[4,15] (iv) The SANS intensity profile at a high concentration (15%) is very similar to the results reported by Wu et al.[18] and Prud'homme et al.[25] The relative peak positions generally observed in concentrated F127/D_2O solutions are $\sqrt{1}$: $\sqrt{3}$: $\sqrt{4}$ with respect to the first-order peak, as shown in Figure 1a. The second-order peak at $\sqrt{2}$ reported by Prud'homme et al.[25] may be smeared with the first-order peak. In our study, we find that SANS itself does not have enough resolution to resolve this second-order peak. Therefore, it is very difficult to determine the microstructure of the gel only from these diffraction peak positions, and the interpretations of the mechanism of gelation are thus very controversial; Wu et al. interpreted the gelation in a F127 aqueous solution as caused by the formation of a face-centered-cubic (*fcc*) gel structure (compact packing of micelle) based on the comparison of the ratio of the peak positions obtained from small-angle X-ray scattering (SAXS) intensity profiles.[18] However, the detailed analysis of the observed SANS scattering patterns by Prud'homme et al.[25] excluded the possibility of *fcc* or lamellar gel-packing geometry. Instead, they suggested that ordered gel structure was due to the cubic packing of spherical micelles. We lean toward Prud'homme's interpretation because the ordered polymeric gel structure can be achieved at a polymer volume fraction of 15%, much lower than the volume fraction of a perfect *fcc* structure (55%) packed gel. This result also may suggest that some solvent molecules will participate in the building of the ordered gel structure formed by polymer networks, resulting in the observation of the waterlike local microviscosity in gel.[24,27] This point has also been mentioned by Mortensen[28] in which the micellar core contains about 30% of water and FTIR studies by Su et al., which suggested that the water content in micellar core decreased as F127 concentration increased.[29] Actually, previous experiments and theoretical calculations suggested that the Pluronic copolymer aqueous solutions usually showed ordered structures with micelle packing. The ordered structures are quite complex and are sensitive to polymer concentration and temperature.[30−32] Because of the conflicting results between SAXS and SANS scattering patterns, and by taking into account the ambiguous peak resolution of the SANS measurements as well as the significantly lower volume fraction of gel compared with a perfect *fcc* structure, we feel that our understanding of the gel structure still may not be conclusive. Instead, our emphasis is to examine the role of bound solvents on the formation of gel network structure.

The temperature-dependent $I(q)$ profiles, as shown in Figure 1b, illustrate that with the increase of temperature, the micelle core sizes slightly increase as the broad shoulders at the q range of 0.1∼0.13 Å^{-1} slightly shift to a lower q, consistent with the previous report.[18] In addition, the micelle structure is almost independent of temperature for temperature up to 65 °C. The further increase of temperature from 65 °C to 80 °C results in a large intermicellar distance, as shown by the peak at 0.03∼0.04 Å^{-1} shifting to a lower q value. Furthermore, the peak at the q range of 0.05∼0.07 Å^{-1} only appears in the temperature range of 30 °C to 50 °C. By taking into account of the phase diagram of F127/ D_2O solutions,[2,19,20,27,33] this result may correspond to the sol−gel transition at the low-temperature range from 22 °C to 30 °C, and a gel−sol transition at the higher temperature range from 50 °C to 60 °C in the 15% F127/D_2O solution. Mortensen and Pedersen[11] published a full review on the mechanism of gelation in Pluronic PEO-PPO-PEO triblock copolymer aqueous solutions more than 10 years ago. The mechanism for these two transitions can be described as the sol−gel transition at the lower temperature was due to the increased packing of micelles, while the gel−sol transition stemmed from phase separation, i.e., the decrease of the hydrated EO units makes the volume fraction of micelle too low to form gel through crowding or jamming.[2,20,25,34−37] The SANS results show a gel region at a relatively lower concentration than those reported in previously published papers.[2,19,20,24,30] We interpret this difference mainly because of two reasons. First is the method to determine the gelling point. The scattering technique is normally more sensitive than rheology, and the critical volume for gelation measured by rheology is consistently higher than that measured by scattering techniques.[37] Second, the D_2O may have a slightly weaker polarity than H_2O, causing the gelation of F127 to occur at a slightly lower concentration.

To clarify the role of solvent on physical gelation, we carry out Monte Carlo simulation to study the effect of bound solvent on the structure of physical gel. To compare with SANS results, the collective structure factor $S(q)$ has been calculated from all the simulation samples through the definition of

$$S(\bar{q}) = \frac{1}{L^3}\sum_r \left(\langle\sigma(\bar{r}')\sigma(\bar{r}'+\bar{r})\rangle - \langle\sigma(\bar{r}')^2\rangle\right)e^{i\bar{r}\cdot\bar{q}} \qquad (1)$$

where $\sigma(\bar{r})$ is the contrast between the sites occupied by copolymer segments and solvents, which is equal to −83.56, −85.03 and 0 ($\times 10^4$ cm^{-2}, taken as unit 1 in the calculation) for A, B, and the free solvent occupied cube, respectively. The magnitude of the structure factor, which represents the Fourier transform of the pair correlation function, is spherically averaged as

$$S(q) = \sum_{|\bar{q}|} S(\bar{q}) / \sum_{|\bar{q}|} 1 \qquad (2)$$

with $q = 2\pi n/L$, where $n = 1, 2, 3, ...$, denotes that, for a given n, a spherical shell is taken as $n - 1/2 \le qL \le n + 1/2$.

On the basis of the contribution to the gel network formation, the solvents in the solutions are categorized into two parts: the free solvent and the bound solvent. The free solvent is normal solvent, and the bound solvent will participate in the building of the ordered gel structure. The bound solvent can be further classified as A site-contacted bound solvent and B site-surrounded bound solvent. The A site-contacted bound solvent arises from the strong attraction interactions including hydrophobic interaction, hydrogen bonding, and the dipole−dipole interaction between A (EO) segment and the solvent (D_2O). The B (PO) site-surrounded bound solvent corresponds to the solvent confined in the hydrophobic micellar core. In the calculation of $S(q)$, the A site-contacted bound solvent and B site-surrounded bound solvent have the same contrast as A and B respectively. For comparison, their contrasts set as the free solvent are also used. Figure 2a shows similar volume fraction dependence of the collective structure factor as that of the angularly averaged scattering intensity profiles shown in Figure

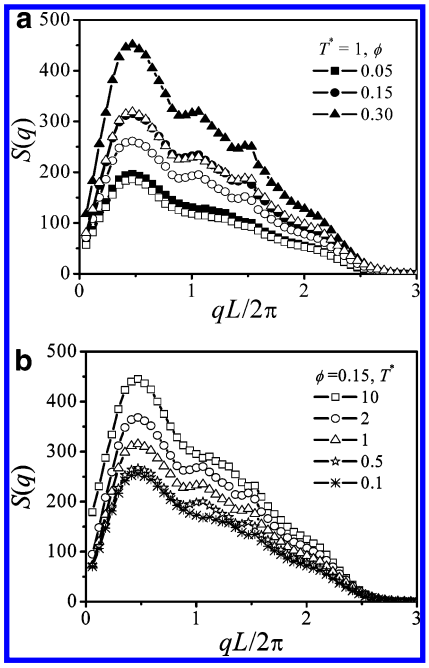

Figure 2. The profiles of the structure factor calculated from Monte Carlo simulation at different volume fractions ($T^* = 0.1$) with (solid) and without (empty) bound solvents (a), and at different reduced temperatures ($\phi = 0.15$) with bound solvent (b).

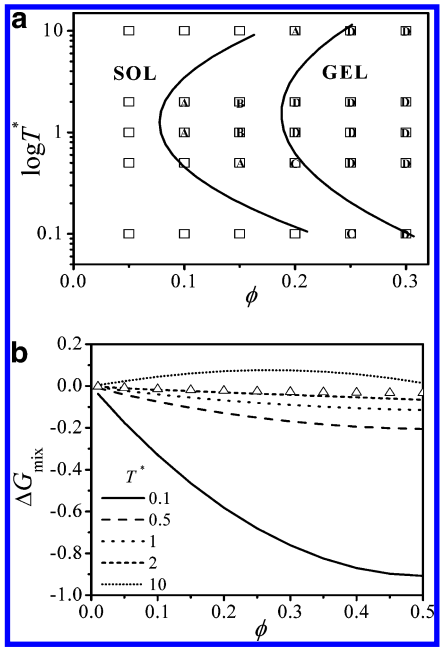

Figure 3. (a) The sol−gel phase diagram from Monte Carlo simulation. The empty squares, A, B, C, and D in the squares represent the probability for the sample to satisfy the two criteria described in experiments and simulations of 0%, 0∼25%, 25∼50%, 50∼75%, and 75∼100% respectively. (b) The plots of the mixing free energy of the polymer solution versus polymer volume fraction at different reduced temperatures. The empty triangles are the pure entropic contribution from eq 2.

1a, in which the scattering intensity $I(q)$ is linearly proportional to the structure factor, which is well known in scattering theory.[14] It is found that the bound solvent strengthens the intensity of $S(q)$ when the polymer volume fraction reaches the critical value of 0.15. Below this critical value, the effect of the bound solvent is negligible. In addition, the higher the polymer volume fraction, the larger the effect of bound solvents will be. However, the collective structure factor with and without bound solvent show similar profiles versus scattering vector, suggesting that the bound solvents do not change the ordered structure in gel. Instead, they only enhance the volume fraction of gel network. Figure 2b shows the temperature dependence of $S(q)$ at the volume fraction of 0.15. One notes that the secondary peak only appears in the intermediate temperature range, consistent with the SANS results (Figure 1b). The intensity of $S(q)$ monotonously increases with temperature because a higher temperature leads to a greater aggregation of B segments. At high temperature (e.g., $T^* = 10$), the secondary peak transforms into a broad shoulder, suggesting the loss of the ordered structure in the gel network. These simulation results are consistent with the SANS data shown in Figure 1b, which may arise from the loss of the bound solvent, or the dehydration of the EO segments suggested by previously published papers.[2,19,20,27,33] Here, we should emphasize that our simulation is not a Reverse Monte Carlo method[38] to re-produce the structure of the sample in scattering experiments. Therefore, the simulation results may show structures slightly different from those obtained from experiments due to the limitation of simulation technology.

To further understand the SANS results, as well as the sol−gel and gel−sol transitions in F127/D_2O solutions, the phase diagram of the simulation systems, which is designed based on the feature of F127/D_2O solution, has been calculated using the method described in our previous work.[15] It is found that the phase diagram from simulation reproduces most of the features reported in experimental results for the F127/D_2O solution,[2,19,20,27,33] as shown in Figure 3a. The temperature-induced sol−gel and gel−sol transitions can be observed by increasing T^* at a given volume fraction larger than 0.1. Our calculation based on Flory's theory[39] shows that the mixing free energy is mainly contributed by the enthalpic term, as evidenced in Figure 3b. The mixing free energy is calculated through

$$\Delta G_{mix} = k_B T\left\{\frac{\phi_A}{N_A}\ln\phi_A + \frac{\phi_B}{N_B}\ln\phi_B + \phi_S\ln\phi_S + \chi_{AS}\phi_A\phi_S + \chi_{BS}\phi_B\phi_S + \chi_{AB}\phi_A\phi_B\right\} \quad (3)$$

where N_A and N_B are the number of segments in A and B blocks, respectively. The Flory interaction parameter χ_{ij} is calculated from $(2\epsilon_{ij} - \epsilon_{ii} - \epsilon_{jj})/2k_BT$, with i, j representing A, B, and S separately. This calculation indicates that the loss of ordered structure at high temperature observed from SANS and $S(q)$ may be derived from phase separation, i.e., the loss of the bound solvent from copolymer chains.

To help understand the temperature-induced sol−gel and gel−sol transitions from the molecular level, the root-mean-square radius of gyration of block A and block B, R_{gA} and R_{gB}, and the ratio, f_{AB}, which is defined as the interaction pairs between A and B segments averaged to each chain divided by the interaction pairs per chain are calculated. Figure 4 reveals three distinct temperature ranges: (1) at $T^* < 0.5$, significant intra-block shrinkage occurs since the R_{gA} and R_{gB} decrease dramatically, and the interaction pair f_{AB} between core and shell (corona) slightly increases; (2) at $0.5 \le T^* \le 2$, the sizes of both A and B blocks slightly increase with temperature. However, f_{AB} increases sharply, suggesting a significant interchain aggregation; and (3) at $2 < T^* \le 10$, R_{gA} and R_{gB} remain nearly constant while f_{AB} continues to increase, suggesting that the interchain continues to aggregate, i.e., the size of micelle continues to increase even when the temperature is sufficiently high, and this trend will result in phase separation as T^* increases. Other parameters such as f_{ii} (f_{AA} or f_{BB}) and the R_g of copolymer chain

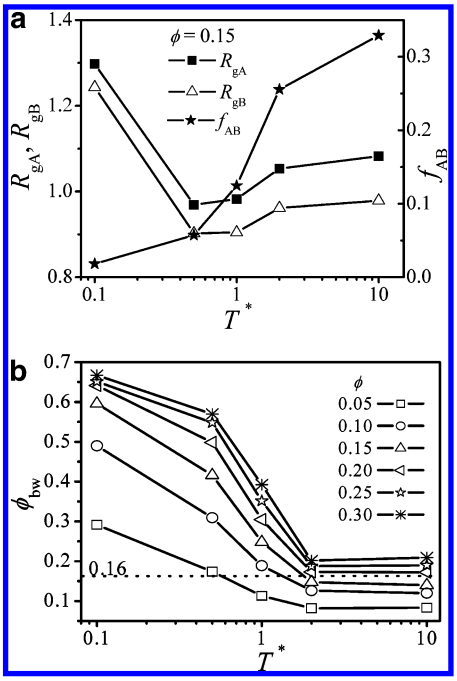

Figure 4. (a) The plot of root-mean-square radius of gyration of block A and block B (R_{gA} and R_{gB}), and the ratio of A-B interaction pairs (f_{AB}) versus reduced temperature. (b) The plots of the total volume fractions of the bound solvent versus reduced temperature at different polymer volume fractions.

have relationships with T^* similar to f_{AB} and R_{gA} (or R_{gB}) respectively at all volume fractions. To better understand the role of bound solvent on physical gelation, the effects of copolymer volume fraction and temperature on the total volume fraction of the bound solvent have been investigated, as shown in Figure 4b. Here, the curves are mainly contributed by the A site-contacted bound solvent, because the volume fraction of all the B site-surrounded bound solvent is smaller than 0.001. One notes that at low temperature (e.g., $T^* = 0.1$), because the solvents are strongly attractive to A segments and slightly repulsive to B segments, the volume fraction of bound solvent ϕ_{bw} is easy to reach the critical value of 0.16.[17] However, at high temperature (e.g., $T^* = 10$), even though the volume fraction of the copolymer approaches the critical value (0.16), ϕ_{bw} is still lower than the critical value. Therefore, we can conclude that at low temperature in which the solvent and A segment in the micellar shell have strong attractive interactions, the physical gelation is dominated by the formation of the percolated polymer network. However, at high temperature, the gel−sol transition is induced by the loss of the bound solvent.

To give an intuitive description for the three different kinds of solvents in F127/D_2O system, the diffusion behaviors of solvent molecules using the parameter of mean-square displacement (MSD) have been studied. The MSD is calculated in the simulation through

$$\mathrm{MSD} = \langle [r(t) - r(0)]^2 \rangle \tag{4}$$

where $r(t)$, which is in the unit of MCS, is the position of a point at the simulation time t. In the calculation of MSD for a polymer chain, the point represents the center of mass of this chain; for a solvent molecule, the point represents the solvent itself. All the diffusion data in this work are collected for an additional 1×10^6 MCS simulation based on the configuration after enough thermodynamic relaxation (5×10^6 MCS). Figure 5 shows the diffusion of three kinds of solvents, i.e., the A site-contacted bound solvent, the B site-surrounded bound solvent, and the free solvent molecules in the gel system mentioned above. The diffusion of A site-contacted bound solvent is similar to that of the free solvent, suggesting that the A site-contacted bound solvent can exchange with the free solvent quickly, because of local thermo or concentration fluctuation. In contrast, the B site-surrounded bound solvent is confined in the micellar core, and it can only diffuse with the diffusion of the whole micellar core, which is certainly much slower than that of a single segment or a free solvent molecule.

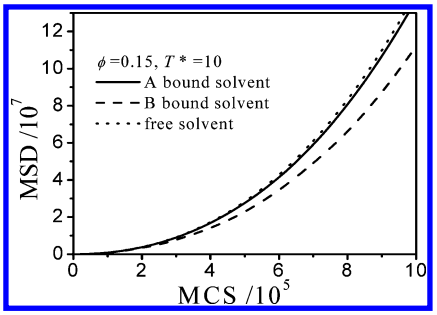

Figure 5. The plots of the MSD of the center of mass of the polymer chain versus MCS with different kinds of solvent ($\phi = 0.15$, $T^* = 10$).

Summary

In summary, we have studied the physical gelation of Pluronic F127/D_2O solutions using small-angle neutron scattering (SANS) and Monte Carlo simulation methods. Our results suggest that the sol−gel transition at low temperature is caused by the formation of percolated polymer network, while the gel−sol transition at a higher temperature is caused by the loss of bound solvents. The bound solvents play an important role in enhancing the volume fraction of micelles, and the three different kinds of solvents diffuse differently in the gel system. The higher the polymer volume fraction, the larger the effect of bound solvents will be. However, the bound solvents do not change the ordered structure of gel. The structure factor profiles calculated from Monte Carlo simulation agree well with the scattering intensity profiles obtained from SANS measurements. In addition, the phase diagram of the F127/D_2O solution also can be successfully reproduced from our simulation. We expect that this general explanation of physical gelation can be further extended to systems with similar sol−gel phase diagrams, although the chemical structure of the polymers may be different.[35,40,41] In addition, the ratio of ϕ_{bw}/ϕ may help to determine and understand the "hard gel" or "soft gel" as well to distinguish a gel, a crystal, or a glass in concentrated polymer solutions.[35,41,42] Finally, the consideration of both the polymer network and the bound solvents may afford some direct information about the structure evolution during flocculation, coacervation, or precipitation processes in many polyelectrolyte complexes.

Acknowledgment. We thank Ed Lang and Dr. Jyotsana Lal at IPNS for their technical support during the SANS measurements. This work was supported by ACS-PRF (41333-G7) (Q.R.H) and the National Natural Science Foundation of China (NSFC) (50373044, 50503022, 50340420392, 20334010, 20490220, 50390090), the National Science Fund for Distinguished Young Investigators (59825113), and the Chinese Academy of Sciences (KJCX2-SW-H07) and subsidized by the Special Funds for Major State Basic Research Projects (No. 2003CB615600, 2005CB623800).

References and Notes

(1) (a) Corriu, R. J. P.; Mehdi, A.; Reyé, C.; Thieuleux, C. *Chem. Commun.* **2003**, 1564. (b) Huang, K.; Lee, B. P.; Ingram, D. R.;

Messersmith, P. B. *Biomacromolecules* **2002**, *3*, 397. (c) Imhof, A.; Pine, D. J. *Nature* **1997**, *389*, 948. (d) Sanchez, C.; Arribart, H.; Madeleine, M.; (e) Guille, G. *Nat. Mater.* **2005**, *4*, 277.

(2) Wu, C.; Liu, T.; Chu, B. *Electrophoresis* **1998**, *19*, 231.

(3) Manley, S.; Wyss, H. M.; Miyazaki, K.; Conrad, J. C.; Trappe, V.; Kaufman, L. J.; Reichman, D. R.; Weitz, D. A. *Phys. Rev. Lett.* **2005**, *95*, 238302.

(4) Chu, B. *Langmuir* **1996**, *11*, 414.

(5) Stauffer, D.; Aharony, A. *Introduction to Percolation Theory*; Taylor & Francis: London, 1992.

(6) Kumar, S. K.; Douglas, J. F. *Phys. Rev. Lett.* **2001**, *87*, 188301.

(7) de Gennes, P. G. *Scaling Concepts in Polymer Physics*; Cornell University Press: Ithaca, NY, 1979.

(8) Thiyagarajan, P.; Epperson, J. E.; Crawford, R. K.; Carpenter, J. M.; Klipper, T. E.; Wozniak, D. G. *J. Appl. Crystallogr.* **1997**, *30*, 280.

(9) Hansen, S.; Pedersen, J. S. *J. Appl. Crystallogr.* **1991**, *24*, 641.

(10) Mortensen, K.; Pedersen, J. S. *Macromolecules* **1993**, *26*, 805.

(11) Anderson, J. A.; Travesset, A. *Macromolecules* **2006**, *39*, 5143.

(12) (a) Deutsch, H. P.; Binder, K. *J. Chem. Phys.* **1991**, *94*, 2294. (b) Li, Y.; Huang, Q.; Shi, T.; An, L. *J. Chem. Phys.* **2006**, *125*, 044902.

(13) Carmesin, I.; Kremer, K. *Macromolecules* **1988**, *21*, 2819.

(14) Higgins, J. S.; Benoît, H. C. *Polymer and Neutron Scattering*; Oxford University Press Inc.: New York, 1994.

(15) Li, Y.; Sun, Z.; Shi, T.; An, L. *J. Chem. Phys.* **2004**, *121*, 1133.

(16) Li, Y.; Sun, Z.; Su, Z.; Shi, T.; An, L. *J. Chem. Phys.* **2005**, *122*, 194909.

(17) (a) Scher, H.; Zallen, R. *J. Chem. Phys.* **1970**, *53*, 3759. (b) Scheffold, F.; Romer, S.; Cardinaux, F.; Bissig, H.; Stradner, A.; Rojas-Ochoa, L. F.; Trappe, V.; Urban, C.; Skipetrov, S. E.; Cipelletti, L.; Schurtenberger, P. *Prog. Colloid Polym. Sci.* **2004**, *123*, 141.

(18) Wu, C.; Liu, T.; Chu, B.; Schneider, D. K.; Graziano, V. *Macromolecules* **1997**, *30*, 4574.

(19) Song, M. J.; Lee, D. S.; Ahn, J. H.; Kim, D. J.; Kimi, S. C. *Polym. Bull.* **2000**, *43*, 497.

(20) Malmsten, M.; Lindman, B. *Macromolecules* **1992**, *25*, 5440.

(21) (a) Chu, B. *Langmuir*, **1995**, *11*, 414. (b) Wu, G.; Chu, B.; Schneider, D. K. *J. Phys. Chem.* **1995**, *99*, 5094.

(22) Pedersen, J. S.; Gerstenberg, M. C. *Macromolecules* **1996**, *29*, 1363.

(23) Mao, G.; Sukumaran, S.; Beaucage, G.; Saboungi, M.-L.; Thiyagarajan, P. *Macromolecules* **2001**, *34*, 552.

(24) Grant, C. D.; DeRitter, M. R.; Steege, K. E.; Fadeeva, T. A.; Castner, Jr. E. W. *Langmuir* **2005**, *21*, 1745.

(25) Prud'homme, R. K.; Wu, G.; Schneider, D. K. *Langmuir* **1996**, *12*, 4651.

(26) Guo, L. Ph.D. Thesis, Pennsylvania State University, University Park, PA, 2003.

(27) Jeon, S.; Granick, S.; Kwon, K. W.; Char, K. *J. Polym. Sci., Part B: Polym. Phys.* **2002**, *40*, 2883.

(28) Mortensen, K. *Polym. Adv. Technol.* **2001**, *12*, 2.

(29) Su, Y.; Wang, J.; Liu, H. *Macromolecules* **2002**, *35*, 6426.

(30) Alexandridis, P.; Olsson, U.; Lindman, B. *Langmuir* **1998**, *14*, 2627.

(31) Noolandi, J.; Shi, A.-C.; Linse P. *Macromolecules* **1996**, *29*, 5907.

(32) Jiang, R.; Jin, Q.; Li, B.; Ding, D.; Shi, A.-C. *Macromolecules* **2006**, *39*, 5891.

(33) Matthew, J. E.; Nazario, Y. L.; Roberts, S. C.; Bhatia, S. R. *Biomaterials* **2002**, *23*, 4615.

(34) Mortensen, K.; Brown, W.; Nordén, B. *Phys. Rev. Lett.* **1992**, *68*, 2340.

(35) (a) Park, M. J.; Char, K. *Langmuir* **2004**, *20*, 2456. (b) Jeong, B.; Windisch, C. F.; Park, M. J., Jr.; Sohn, Y. S.; Gutowska, A.; Char, K. *J. Phys. Chem. B* **2003**, *107*, 10032.

(36) Grant, C. D.; Steege, K. E.; Bunagan, M. R.; Castner, Jr. E, W. *J. Phys. Chem. B* **2005**, *109*, 22273.

(37) *Faraday Discuss.* **2003**, *123*, 75.

(38) Misawa, M. *J. Chem. Phys.* **2002**, *116*, 8463.

(39) Rubinstein, M.; Colby, H. *Polymer Physics*; Oxford University Press: New York, 2004.

(40) (a) Hvidt, S.; Jøgensen, E. B.; Brown, W.; Schillén, K. *J. Phys. Chem.* **1994**, *98*, 12320. (b) Nyström, B.; Walderhaug, H. *J. Phys. Chem.* **1996**, *100*, 5433. (c) Bae, S. J.; Suh, J. M.; Sohn, Y. S.; Bae, Y. H.; Kim, S. W.; Jeong, B. *Macromolecules* **2005**, *38*, 5260.

(41) Crothers, M.; Attwood, D.; Collett, J. H.; Yang, Z.; Booth, C.; Taboada, P.; Mosquera, V.; Ricardo, N. M. P. S.; Martini, L. G. A. *Langmuir* **2002**, *18*, 8685.

(42) (a) Ricardo, N. M. P. S.; Honorato, S. B.; Yang, Z.; Castelletto, V.; Hamley, I. W.; Yuan, X.-F.; Attwood, D.; Booth, C. *Langmuir*, **2004**, *20*, 4272. (b) Park, M. J.; Char, K.; Kim, H. D.; Lee, C.; Seong, B.; Han, Y. *Macromol. Res.* **2002**, *10*, 325. (c) Hamley, I. W.; *Philos. Trans. R. Soc. London, Ser. A* **2001**, *359*, 1017. (d) Hamley, I. W.; Mai, S.-M.; Ryan, A. J.; Fairclough, J. P. A.; Booth, C. *Phys. Chem. Chem. Phys.* **2001**, *3*, 2972.